Journal of Inorganic Biochemistry 186 (2018) 135–146

Contents lists available at ScienceDirect

Journal of Inorganic Biochemistry

journal homepage: www.elsevier.com/locate/jinorgbio

In-vivo evaluation of the response of *Galleria mellonella* larvae to novel copper(II) phenanthroline-phenazine complexes

Garret Rochford[a,*], Zara Molphy[b], Niall Browne[c], Carla Surlis[c], Michael Devereux[a], Malachy McCann[d], Andrew Kellett[b], Orla Howe[a], andKevin Kavanagh[c]

[a] Centre for Biomimetics and Therapeutics and Focas Research Institute, Dublin Institute of Technology, Camden Row, Dublin 8, Ireland
[b] School of Chemical Sciences and National Institute for Cellular Biotechnology, Dublin City University, Dublin 9, Ireland
[c] Department of Biology, Maynooth University, Maynooth, Co. Kildare, Ireland
[d] Department of Chemistry, Maynooth University, Maynooth, Co. Kildare, Ireland

ARTICLE INFO

Keywords:
Chemical nuclease
Copper phenanthrene
Galleria mellonella
in-vivo toxicity
DNA
LFQ proteomics

ABSTRACT

Herein we report the *in-vivo* characterisation and metabolic changes in *Galleria mellonella* larvae to a series of bis-chelate copper(II) phenanthroline-phenazine cationic complexes of $[Cu(phen)_2]^{2+}$ (Cu-Phen), [Cu(DPQ)(Phen)]$^{2+}$ (Cu-DPQ-Phen) and [Cu(DPPZ)(Phen)]$^{2+}$ (Cu-DPPZ-Phen) (where phen = 1,10-phenanthroline, DPQ = dipyrido[3,2-*f*:2′,3′-*h*]quinoxaline and DPPZ = dipyrido[3,2-*a*:2′,3′-*c*]phenazine). Our aim was to investigate the influence of the systematic extension of the ligated phenazine ligand in the *G. mellonella* model as a first step towards assessing the *in-vivo* tolerance and mode of action of the complex series with respect to the well-studied oxidative chemical nuclease, Cu-Phen. The Lethal Dose$_{50}$ (LD_{50}) values were established over dose ranges of 2 – 30 μg at 4-, 24-, 48- and 72 h by mortality assessment, with Cu-Phen eliciting the highest mortality at 4 h (Cu-Phen, 12.62 μg < Cu-DPQ-Phen, 21.53 μg < Cu-DPPZ-Phen, 26.07 μg). At other timepoints, a similar profile was observed as the phenazine π-backbone within the complex scaffold was extended. Assessment of both cellular response and related gene expression demonstrated that the complexes did not initiate an immune response. However, Label-Free Quantification proteomic data indicated the larval response was associated with upregulation of key proteins such as Glutathione *S*-transferase, purine synthesis and glycolysis/gluconeogenesis (*e.g.* fructose-bisphosphate aldolase and glyceraldehyde-3-phosphate). Both Cu-Phen and Cu-DPQ-Phen elicited a similar *in-vivo* response in contrast to Cu-DPPZ-Phen, which displayed a substantial increase in nitrogen detoxification proteins and proteins with calcium binding sites. Overall, the response of *G. mellonella* larvae exposure to the complex series is dominated by detoxification and metabolic proteome response mechanisms.

1. Introduction

Almost 40 years since receiving Federal Drug Administration (FDA) approval, cisplatin still remains one of the most important chemotherapies available today for the combination treatment of cancers including metastatic testicular and ovarian cancers, bladder and lung. However, dose limiting side effects including neurotoxicity and nephrotoxicity and the development of both acquired and inherently resistant cancers continue to be an ongoing issue in its treatment success. As such, recent research activity has focused on the rational design of metallo-agents including ruthenium [1–5], iron [6, 7], gold [8–10] and copper [11–19] with alternative mode of action to the mono-nuclear cis-[PtX_2(amine)$_2$] chemotype (X = leaving group, amine = neutral or carrier group) shared by cisplatin and its derivatives [20].

Copper is an endogenous metal ion that plays an essential role in the structure and activity of multiple functional protein classes, such as enzymes designated to detoxification and oxidative phosphorylation. The essential nature of copper in the cell and its complex homeostasis through specific transporters and trafficking proteins; Copper Transporter 1/2 (CRT1 and CRT2), ATPase copper transporting 7 alpha/beta (ATP7α and ATP7β) holds a strong potential for the utilisation of copper as part of a metallodrug [21].

The therapeutic development of copper complexes has progressed to an advanced stage with two members of the Reactive Oxygen Species (ROS)-active, mixed chelate Casiopeinas® class recently entering phase I clinical trials [22]. The compounds have previously shown antiproliferative and antitumoural effects in medulloblastoma [23], glioma [24] and colorectal adenocarcinoma [25] cell lines. Their mechanism of

* Corresponding author.
E-mail address: garret2400@gmail.com (G. Rochford).

https://doi.org/10.1016/j.jinorgbio.2018.05.020
Received 1 December 2017; Received in revised form 15 May 2018; Accepted 27 May 2018
Available online 01 June 2018
0162-0134/

Abbreviations

2D PAGE	2 dimensional poly acrylamide gel electrophoresis
AICAR	transformylase-phosphoribosylaminoimidazolecarboxamide formyltransferase
ATP7A/B	ATPase copper transporting alpha/beta
CTR1/2	Copper Transporter 1/2
DMSO	Dimethyl Sulfoxide
DNA	Deoxyribonucleic Acid
DTT	Dithiothreitol
FDA	Federal Drug Administration
FDR	false discovery rate
GO	Gene Ontology
GST	Glutathione *S*-transferase
HSP	Heat Shock Protein
IAA	Iodoacetamide
IMPI	Inducible of Metalloproteinase Inhibitor
KEGG	Kyoto Encyclopedia of Genes and Genomes
LD_{50}	Lethal Dose (50%)
LFQ	Label Free Quantitative (proteomics)
MDR	Multi Drug Resistance
mRNA	messenger Ribonucleic Acid
NAD	Nicotinamide Adenine Dinucleotide
NCI DTP	National Cancer Institute Developmental Therapeutics Program
PCA	principle component analysis
qRT-PCR	quantitative Real-Time Polymerase Chain Reaction
ROS	Reactive Oxygen Species
SAICAR synthase	phosphoribosylaminoimidazole-succinocarboxamide synthase
SBC3	1,3-dibenzyl-4,5-diphenyl-imidazol-2-ylidene silver(I) acetate
SOD	Superoxide Dismutase
TCA	Tricarboxylic Acid (cycle)

action is not fully understood, however they are believed to exert their biological effects through (i) binding Deoxyribonucleic Acid (DNA) with intercalative and non-intercalative methods at high affinities, (ii) degrading nucleic acids through the generation of ROS and depleting the antioxidant systems, and (iii) inducing mitochondrial toxicity [26]. Further examples of ternary mixed ligand chelated copper (II) complexes include a developmental therapeutic [Cu(*o*-phthalate)(1,10-phenanthroline)]$^{2+}$ encorporating a bis-chelate dicarboxylate and *N,N′*-intercalative square planar coordination scaffold that has recently shown endogenous ROS production inducing DNA damage and mitochondrial depolarisation resulting in apoptotic induction [16]. Furthermore, the cytotoxic profile of the complex within the National Cancer Institute (NCI) Developmental Therapeutics Program (DTP) 60 human cancer cell panel revealed a novel mode of action to existing metal-based therapeutics.

At the heart of the promising chemotherapeutic potential exerted by many copper(II) complexes lies the artificial metallo-nuclease activity of the parent copper(II) bis-1,10-phenanthroline (Cu-Phen) agent [27]. Evidence suggests the complex binds DNA predominately in the minor groove and in its reduced form abstracts a hydrogen atom primarily from the C1′ deoxyribose position resulting in strand damage [28, 29], with di-copper chemotypes demonstrating singlet oxygen and superoxide production [30]. However, the nuclease binds both nucleic acids and proteins without specificity inducing general toxicity, and is thus considered a “promiscuous” agent [31]. Accordingly, manipulation of this chemotype represents an interesting developmental challenge. With this in mind, a range of novel Cu(II) chemical nucleases of [Cu(phen)(*N,N′*)]$^{2+}$ carrying designer phenazine type-intercalators (where *N,N′* represents phen = 1,10-phenanthroline, DPQ = dipyrido[3,2-*f*:2′,3′-*h*]quinoxaline and DPPZ = dipyrido[3,2-*a*:2′,3′-*c*]phenazine) were developed by Molphy et al. to identify how the systematic extension of the ligated phenanthrene ligand influences nucleotide binding affinity, base selectivity, oxidative chemical nuclease activity, and cytotoxicity within human cancer cells [32]. Agents within this series showed potent intercalative selectivity, high-affinity duplex-DNA binding constants and significant *in-vitro* cytotoxicity in the SKOV3 cisplatin-resistant ovarian cell line.

Galleria mellonella larvae have become an important model for studying human pathogens in addition to being an evaluative mechanism for antimicrobial and antifungal testing [33–36]. A number of factors contribute to this Lepidoptera species being a viable screening model such as: the possession of a similar humoral and cellular immune response to mammals [35, 37], the ability to incubate pathogens at human physiological temperature [34], the physical size of the larvae allowing for ease of inoculation and visual effects being readily observable [38], and having lower ethical and financial restrictions associated with their use [39]. Haemocyte-mediated ROS production has been proposed to be central to the immune response of *G. mellonella* [40]. Several genes have been found to be up regulated during infection and provide a good indicator of the immunogenic nature of the insult on the larvae [41]. Several studies examining toxicities and assessing larval tolerance have been undertaken against a range of metal complexes. The cytotoxicity and subsequent biological activity of Cu(II) 1, 10-phenanthroline and Cu(II) 1, 10-phenanthroline-5,6-dione was well tolerated by the larvae in addition to showing strong *in-vitro* activity in mammalian cells lines [42]. A further study involving a series of Imidazole Schiff base ligands complexed to Ag(I), Cu(II) and Zn(II) were shown to be well tolerated in *G. mellonella* larvae [43]. A subsequent study showed the tolerance of larvae to Ag(I) carbine complex provided an opportunity to assess the antimicrobial activity which showed increased survival following infection with *Candida albicans* [44]. *G. mellonella* larvae have also demonstrated a high degree of tolerance to both Cu^{2+} 1, 10-phenanthroline octanedionate and Mn^{2+} 1, 10-phenanthroline octanedionate complexes [45]. A mechanistic study of this nature would help provide key insights into the activity and potential molecular targets of Cu(II) phenanthroline-phenazine complexes in an *in-vivo* context and aid in future biological testing.

Given the promising activity of Cu(II) phenanthroline-phenazine complexes, [32, 46] the current study seeks to characterise the *in-vivo* toxicity, immune related gene expression and proteomic effects of Cu-Phen, Cu-DPQ-Phen and Cu-DPPZ-Phen in *G. mellonella* larvae. Proteomic responses were recorded through Label Free Quantification (LFQ) in addition to 2-Dimensional Polyacrylamide gel electrophoresis (2D PAGE) methods. LFQ allows a high-resolution assessment of the proteomic changes in the larvae and is becoming an increasingly important tool in identifying the mode of action in *in-vitro* mammalian cell models [47, 48]. Owing to the similarity between the larval and mammal system, this approach will provide valuable insights into the potential mode of action of the phenazine-functionalised Cu(II) phenanthroline complexes in mammalian models.

2. Materials and methods

2.1. Preparation of Cu(II) complexes

Cu-Phen (**1**), Cu-DPQ-Phen (**2**) and Cu-DPPZ-Phen (**3**) (Fig. 1) were synthesised and characterised as previously described [32]. Complexes were initially dissolved in Dimethyl Sulfoxide (DMSO) (Sigma, Ireland) followed by dilution in working aqueous solution. Individual doses were made up in sterile water from the stock solution producing a range between 1500 and 200 μg cm^{-3}.

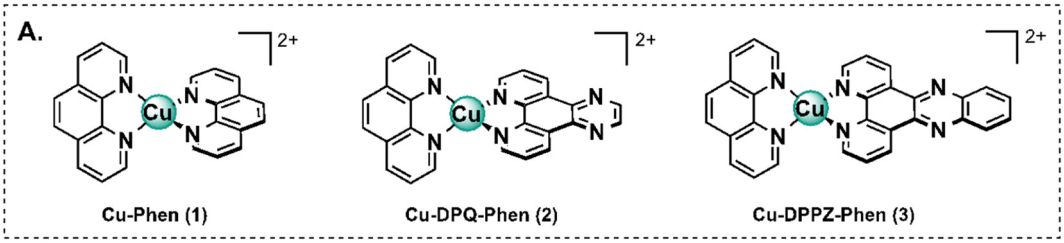

Fig. 1. Molecular structure of Cu(II) coordination complexes (**1**–**3**).

2.2. Galleria mellonella mortality and haemocyte density assessment

Galleria mellonella larvae of the 6th instar development stage were sourced from Livefoods Direct Ltd. (Sheffield, England) and were stored in the dark at 15 °C in wood shavings prior to testing. Thirty three larvae for each replicate (11 × 3) (average weight 0.3 ± 0.05 g) with no cuticle decolouration were used for each experimental condition. All test solutions were prepared immediately prior to testing. Larvae were inoculated with 20 µL of the test complex [49]. A solvent control (8.94% DMSO) in Sterile MilliQ water was inoculated along with sham-inoculations and undisturbed controls. Larval mortality was recorded over 72 h after incubation at 30 °C. The lethal dose (LD) concentration inducing 50% larval death (LD_{50}) for each timepoint was calculated using non-linear regression analysis (GraphPad Prism ver. 5.0). Haemocyte density assessment was determined [50] after inoculation with the 24 h LD_{50} exposures. The exposure was performed on 4 independent occasions, utilising 5 larvae per exposure. Haemocyte density was represented by mean ± standard deviation.

2.3. Induction of IMPI and transferrin by quantitative Real Time – PCR (qRT-PCR)

Inducible metalloproteinase inhibitor (IMPI) and transferrin are commonly seen to be raised in insect based immune reactions [51, 52]. IMPI and transferrin (Table 1) were therefore assessed for their expression relative to the reference gene S7e (ribosomal subunit) after larvae were inoculated with the 24 h LD_{50} value of Cu-Phen (**1**), Cu-DPQ-Phen (**2**) and Cu-DPPZ-Phen (**3**). Controls for the solvent, injection (sham-inoculation) and temperature (undisturbed) were included in the assessment. Total RNA was extracted from the larvae by snap freezing (liquid nitrogen) 3 larvae (representative of each condition) as previously described [53]. qRT-PCR was performed on the 7500 Real-Time PCR system (Applied Biosystems®) using SYBR FAST qPCR kit (KAPA Biosciences) (See S-1 for parameters).

2.4. Label free quantification (LFQ) - proteomics

Larvae were inoculated with the 24 h LD_{50} values of Cu-Phen (**1**) (8.94 µg), Cu-DPQ-Phen (**2**) (11.47 µg), Cu-DPPZ-Phen (**3**) (25.05 µg) and solvent control (8.94% DMSO in MilliQ grade water). Haemolymph protein from 5 pooled (performed 4 independent times) larvae were extracted and quantified using the Bradford method [55]. Samples were normalized to 100 µg prior to reduction with dithiotreitol (DTT; 200 mM), followed by alkylation with iodoacetamide (IAA; 1 M) and digested with sequence grade trypsin (Promega, Ireland) at a ratio of 1:40 trypsin to protein over night at 37 °C. Prior to C18 column clean-up, samples were separated by 1 Dimensional (1D) gel electrophoresis along with a size ladder and stained with coomassie blue to verify the presence and quantity of proteins in the samples. Following verification, samples were subjected to a clean-up procedure utilising C18 columns with spin filters (Medical Supply Company, Ireland). Peptide mix was separated on a Dionex Ultimate 3000 (RSLC nano) chromatography system with increasing gradient of acetonitrile on a Biobasic C18 PicofritTM column (100 mm length, 75 mm ID), using a 60 min reverse phase gradient at a flow rate of 250 nL min^{-1}. High-resolution Mass Spectrometry (MS) (300–2000 Da) was performed using the Q Exactive (ThermoFisher, USA) to select the 15 most intense ions prior to MS/MS Q. Protein spots identified in the 2-Dimensional Polyacrylamide Gel Electrophoresis (2D PAGE) analysis (see S-1 for details) were excised and trypsin digested similarly to the method described. [56]

Proteins were identified through the Andromeda search engine [57] in MaxQuant (ver. 1.2.2.5, http://maxquant.org/) to correlate the data against a 6-frame translation of the expressed sequence tag contigs identified from complementary DNA (cDNA) for *G. mellonella* [58]. First search peptide tolerance of 20 ppm was followed by the second search peptide tolerance of 4.5 ppm with cysteine carbamidomethylation as a fixed modification, *N*-acetylation of protein and oxidation of methionine as variable modification, and a maximum of 2 missed cleavage sites allowed. False discovery rate (FDR) was set to 1% for both peptides and proteins and FDR was estimated following searches against a target decoy database. Peptides with a minimum length of seven amino acids were considered for identification and proteins were only considered identified when more than one unique peptide for each protein was observed.

2.5. Statistical analysis

Larval mortality was used to establish LD_{50} using non-linear regression analysis (GraphPad Prism, ver. 5.0). Gene expression was assessed through the use of relative expression to the reference gene S7e and was technically replicated on four occasions. Analysis of critical threshold values was performed as per Livak and Schmittgen relative expression method [59]. LFQ proteomics was run on 4 separate occasions with Sodium Dodecyl Sulfate Polyacrylamide Gel Electrophoresis (SDS PAGE) used to check the integrity of samples prior to Liquid Chromatography/Mass Spectrometry (LC/MS) injection. Statistical and graphical analysis of the LFQ proteomics was performed using Perseus

Table 1
Sequence of primers for IMPI and transferrin.

Gene (primers)	Oligonucleotides sequence (5′-3′)	Fragment size (base pair (bp))	Reference	Function (encodes)
S7e F	ATGTGCCAATGCCCAGTTG	131	[54]	Structural ribosomal protein
S7e R	GTGGCTAGGCTTGGGAAGAAT			
Transferrin F	CCCGAAGATGAACGATCAC	535	[41]	Iron transport and binding
Transferrin R	CGAAAGGCCTAGAACGTTTG			
IMPI F	ATTTGTAACGGTGGACACGA	409	[41]	Inhibits pathogen secreted enzymes
IMPI R	CGCAAATTGGTATGCATGG			

v. 1.5.0.31. Log2 –transformation was performed on all LFQ intensities that met the identification criteria with subsequent ANOVA of significance and *t*-tests between the solvent control and the test complexes exposures. The *p*-value of 0.05 was set with significance determined using FDR correction (Benjamini-Hochberg). Proteins were only included when they were present in at least 3 of 4 biological replicates. Proteins which had LFQ intensity values of zero (indicating absence or low abundance) were included in the study only when the protein was absent in one group and present in at least three replicates of another group. Imputation was used to correct for missing identifications in samples based on Gaussian distribution using the lowest value for each dataset, which was calculated as being 1.75 downshift from the mean value and 0.25 width in the downshift for the standard deviation. The Blast2GO suite (www.blast2GO.com) of software tools was used to assign annotation, enzyme code, Kyoto Encyclopedia of Genes and Genomes (KEGG) and Gene Ontology (GO) mapping. GO mapping for biological processes and molecular functions was graphed at level 4 ontology.

3. Results

3.1. Larval mortality assay and haemocyte count

G. mellonella larvae were administered with Cu-Phen (**1**), Cu-DPQ-Phen (**2**), Cu-DPPZ-Phen (**3**) and cisplatin with the level of toxicity being assessed by the mean mortality (%) over 72 h (Supplementary Table I and II). No mortality (data not shown) was recorded at any timepoint after incubation of solvent (8.94% DMSO in MilliQ water), sham inoculated and undisturbed controls. The results of the individual larval responses to the inoculated doses and timepoints are detailed in S-1. The LD_{50} values (Table 2) from Cu-Phen (**1**), Cu-DPQ-Phen (**2**) and Cu-DPPZ-Phen (**3**) decrease over the increasing timepoints with Cu-Phen (**1**) showing superior toxicity to both Cu-DPQ-Phen (**2**) and Cu-DPPZ-Phen (**3**) at all timepoints. Haemocytes were numerated from the haemolymph extracted from 5 larvae per treatment (LD_{50} value at 24 h) with this procedure replicated 4 times (for statistical validity). No significant changes (data not shown) were observed between any of the controls and test complex exposures.

3.2. Induction of IMPI and transferrin assessed by qRT-PCR

Larvae were exposed to the 24 h LD_{50} value of Cu-Phen (**1**), Cu-DPQ-Phen (**2**) and Cu-DPPZ-Phen (**3**). Solvent control, sham-inoculation and undisturbed control were utilised as previously described. Both transferrin and IMPI were normalized against the expression of S7e reference gene and all larval treatments were compared to the solvent control. Both sham-inoculation and undisturbed controls produced similar expression levels (data not shown). Fig. 2 demonstrates the expression of both genes. A significant decrease in IMPI expression (Fig. 2) was observed in Cu-Phen (**1**), Cu-DPQ-Phen (**2**) and Cu-DPPZ-Phen (**3**) treated larvae in comparison to the solvent control. In all LD_{50} complex exposures a significant decrease in transferrin activity (Fig. 2) was observed with respect to the solvent control. The solvent control demonstrated decreased expression in both measured genes in relation to the undisturbed biological control.

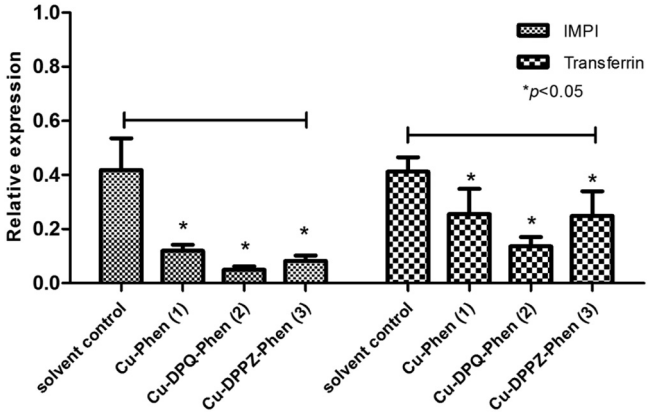

Fig. 2. Relative expression of IMPI and transferrin after 24 h exposure to LD_{50} value of Cu-Phen (**1**), Cu-DPQ-Phen (**2**) and Cu-DPPZ-Phen (**3**). Gene expression is displayed relative to the undisturbed control with the solvent control used to determine significance ($p < 0.05$).

3.3. Label free quantification (LFQ) – Proteomics between test exposures and control

The haemolymph of larvae was extracted after the 24 h exposure to the LD_{50} value of the complex series in order to assess the difference in protein abundance between the treated and control larvae. A total of 299 proteins were detected with 2 or more peptides. One hundred and four proteins were found to be significantly altered in abundance or uniquely detected across the 4 conditions (Table 3). Nine proteins were found to be absent or below the limit of detection following exposure to Cu-DPQ-Phen (**2**). Twelve proteins were found to be absent or below the detection limit following exposure to Cu-Phen (**1**). Four proteins were found to be absent or below the limit of detection after exposure to Cu-DPQ-Phen (**2**) and Cu-DPPZ-Phen (**3**). One protein was found to be absent or below the limit of detection after exposure to Cu-Phen (**1**) and Cu-DPPZ-Phen (**3**). Twenty-three proteins were found to be absent or below the limit of detection after exposure to Cu-Phen (**1**) and Cu-DPQ-Phen (**2**). Table 3 demonstrates increasing numbers of significantly up regulated proteins in the following pattern: Cu-Phen (**1**) < Cu-DPQ-Phen (**2**) < Cu-DPPZ-Phen (**3**). In the case of Cu-DPPZ-Phen (**3**) exposure, a greater number of antimicrobial proteins were observed to be significantly down regulated while a greater number of metabolic proteins and proteins containing calcium binding sites were up regulated. Principle component analysis (PCA) (Fig. 3) was used to visualise the variation in protein abundance across the individual replicates. The proteomes of larvae exposed to the solvent control and Cu-DPPZ-Phen (**3**) showed clustering that was widely separated by component 1 (greatest measure of profile divergence), however Cu-Phen (**1**) and Cu-DPQ-Phen (**2**) were closely clustered, indicating a similar protein expression profile. Hierarchical clustering (Supplementary Fig. 2) similarly reflected the PCA. Four replicates were included for the solvent control and one replicate was removed from each of the test exposures due to lack of clustering with the parent group. GO terms were categorised by both biological processes (Fig. 4(A)) and molecular

Table 2
Calculated LD_{50} values. * Cu-DPPZ-Phen (**3**) injected in micro-suspension.

Compounds	LD_{50} (μg) ± S.D			
	4 h	24 h	48 h	72 h
Cu-Phen (1)	12.62 ± 0.008	8.94 ± 0.006	8.94 ± 0.006	8.56 ± 0.75
Cu-DPQ-Phen (2)	21.53 ± 0.007	11.47 ± 0.006	10.69 ± 0.005	9.88 ± 0.017
Cu-DPPZ-Phen (3)*	26.07 ± 0.312	25.05 ± 0.312	25.05 ± 0.312	16.81 ± 0.236

Table 3
Statistically Significant Differentially Abundant (SSDA) proteins present in Cu-Phen (**1**), Cu-DPQ-Phen (**2**) and Cu-DPPZ-Phen (**3**) in comparison to the solvent control. Relative fold changes are given for each complex exposure in comparison to the solvent control.

Protein annotation	Relative expression to solvent control		
	Cu-Phen (**1**)	Cu-DPQ-Phen (**2**)	Cu-DPPZ-Phen (**3**)
Aldehyde dehydrogenase mitochondrial-like	2.19	7.16	8.05
Selenium-binding 1	2.02	6.62	7.8
Lambda-crystallin homolog	4.89	6.76	7.55
Tubulin beta chain	4.64	6.37	7.41
D-arabinitol dehydrogenase 1-like	5.24	5.8	6.85
Elongation factor 1-alpha	6.19	5.57	6.63
15-hydroxyprostaglandin dehydrogenase [NAD(+)]-like	2.96	5.05	6.49
Cytoplasmic A3a	1.28	5.74	6.4
N-acetylneuraminate lyase-like	5.17	5.69	6.38
Serine cytosolic isoform X1	0.63	5.48	6.36
Multifunctional ADE2	5.13	5.13	6.19
Cytosolic malate partial	2.81	4.97	6.16
D-3-phosphoglycerate dehydrogenase	3.05	5.27	6.04
Glutathione *S*-transferase-like	5.18	4.65	5.99
Tubulin alpha chain	4.68	4.6	5.9
Triosephosphate isomerase	4.92	4.96	5.87
Glutamine synthetase 2 cytoplasmic-like	3.61	5	5.41
Probable enoyl- mitochondrial	1.09	4.61	5.31
Glutathione *S*-transferase 1-1-like	2.78	4.6	5.22
Glyceraldehyde-3-phosphate partial	3.14	4.6	5.04
Fructose-bisphosphate aldolase isoform X1	4.59	4.14	4.94
Superoxide dismutase [Mn] mitochondrial	−1.52	3.53	4.7
Trans-1,2-dihydrobenzene-1,2-diol dehydrogenase-like	4.69	4.17	4.7
Bifunctional purine biosynthesis PURH	1.75	3.7	4.56
Aminopeptidase	1.39	3.34	4.39
Heat shock 90	3.39	3.36	4.33
Enolase	3.49	2.95	4.32
L-threonine ammonia-lyase-like	4.08	3.3	4.27
Arginine partial	4.02	2.04	4.24
Aliphatic nitrilase	3.61	3.19	4.19
Dihydropteridine reductase	6.24	3.4	4.13
Peptidyl-prolyl *cis-trans* isomerase	3.03	3.12	4.13
Cholinesterase 1-like	6.1	3.64	4.02
Purine nucleoside phosphorylase	3.49	1.96	3.97
Cellular retinoic acid binding	5.01	3.06	3.77
Argininosuccinate synthase	1.28	2.66	3.74
Uncharacterized protein Dmoj_GI19595	2.25	1.91	3.65
Immune-related Hdd1	4.43	3.58	3.57
Ejaculatory bulb-specific 3-like	2.05	3.68	3.52
Fibrous sheath CABYR-binding	5.16	2.89	3.46
Leukotriene A-4 hydrolase isoform X2	2.13	3.26	3.13
PREDICTED: uncharacterized protein LOC106129042	3.89	3.23	3.13
Ecdysteroid-regulated 16 kDa -like	2.54	3.23	2.64
Isopentenyl-diphosphate Delta-isomerase 1	−1.01	2.13	2.55
Heat shock	1.98	2.2	2.4
Proliferation-associated 2G4	2.61	1.98	2.35
Seroin-like isoform X2	−2.06	1.37	2.28
Actin	1.63	4.22	1.99
Nucleoside diphosphate kinase	−0.66	0.79	1.83
Chitin deacetylase 1	6.88	1.52	1.55
Contig19736_1_exp_NA	1.43	−1.62	−1.82
Homeobox 2-like isoform X4	3.15	−1.33	−2.15
Probable salivary secreted peptide	2.9	−1.72	−2.8
Gloverin-like	0.92	−2.5	−2.96
Peptidoglycan recognition	2.03	−4.02	−3.28
Glutathione *S*-transferase 1-like	5.11	–	4.67
Profilin	3.18	–	3.64
Aminoacrylate peracid reductase	−0.69	–	3.35
Cytosolic non-specific dipeptidase	2.23	–	3.1
Circadian clock-controlled -like	3.01	–	2.7
4-Coumarate—ligase 1-like	1.16	–	2.62
Multiple inositol polyphosphate phosphatase 1-like	1.14	–	1.86
Isocitrate partial	2.7	–	1.48
Esterase FE4-like	5.06	–	−1.18
Thioredoxin	–	3.87	4.81
Rab GDP dissociation inhibitor alpha	–	3.15	4.55
Probable phosphoserine aminotransferase	–	4.23	4.46
Small heat shock	–	3.46	3.97
Takeout-like	–	2.33	3.97
High mobility group D	–	2.27	3.74
Staphylococcal nuclease domain-containing 1	–	2.13	3.16
Glutathione *S*-transferase omega 1	–	2.07	2.92
Fumarylacetoacetase	–	1.57	2.35
Hydroxypyruvate isomerase	–	1.1	1.76
Apolipophorins isoform X2*	–	−4.15	−0.72
Chitinase EN03 (imaginal disc growth)*	–	−0.72	−1.5
Translationally controlled tumor	5.64	–	–
Cysteine ase inhibitor precursor	2.71	–	–
Gustatory receptor candidate 59	2.5	–	–
Chemosensory	2.48	–	–
Serpin-2	–	2.00	–
Muscle-specific 20	–	–	5.73
Peroxiredoxin- mitochondrial	–	–	4.96
Tropomyosin-1 isoform X1	–	–	4.22
Troponin T	–	–	4.18
Annexin B9 isoform X4	–	–	4.15
Troponin I	–	–	3.97
Asteroid	–	–	3.62
Antichymotrypsin-2-like isoform X2	–	–	3.56
Ubiquitin carboxyl-terminal hydrolase isozyme L3	–	–	3.14
S-Adenosyl-L-homocysteine partial	–	–	3.08
C-1-tetrahydrofolate cytoplasmic isoform X2	–	–	3.03
Troponin C	–	–	2.88
Phosphoglycerate mutase 1	–	–	2.82
Probable transaldolase	–	–	2.78
ATPase inhibitor	–	–	2.28
Acyl-binding homolog	–	–	1.99
Proactivator polypeptide	–	–	1.74
Phosphotriesterase-related -like	–	–	1.71
L-threonine 3- mitochondrial	–	–	1.66
Prostaglandin reductase 1	–	–	1.57
Vanin 2 isoform X1	–	–	−1.79
Chymotrypsin-like elastase family member 2A	–	–	−2.3
Serine protease 42-like	–	–	−2.41

- denotes level of expression that was either absent or not detected. Fold changes of $^{<}1.5$ were included when expression in other test exposures was ≥ 1.5 fold change. *Denotes protein also expressed in 2D PAGE analysis with a similar profile, see Supplementary Table III. Numerical difference between the detected proteins between the two proteomics methods was due to the greater sensitivity of LFQ proteomics method.

function (Fig. 4(B)) with categorisations being performed at level 4 ontology. The biological process analysis (Fig. 4(A)) does not show any major changes in larvae inoculated with the different complexes. Protein groups such as precursor metabolites, organonitrogen and cellular nitrogen associated proteins were more prominent in terms of observed proteins. An overall increase was observed in the number of proteins recorded after exposure to Cu-DPQ-Phen (**2**) and Cu-DPPZ-Phen (**3**) with the number of proteins increasing as the ligated phenazine π-backbone was extended. However, the number of proteins associated with each GO process proportionally increased in comparison to Cu-Phen (**1**). Interestingly, proteins associated with sulphur compounds and cellular aldehyde processes were only present after exposure to Cu-

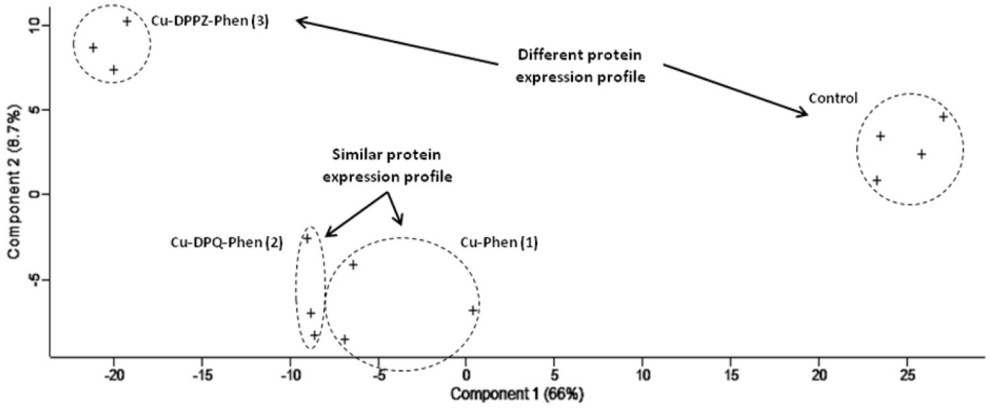

Fig. 3. Principle component analysis (PCA) of haemolymph proteomic profiles of larvae inoculated with Cu-Phen (**1**), Cu-DPQ-Phen (**2**) and Cu-DPPZ-Phen (**3**) *versus* the solvent control. PCA of four replicates for the solvent control and three replicates for each of the test exposures. Enclosures define the different experimental conditions. Component 1 on the x-axis represents the largest difference in terms of protein expression profile with Component 2 on the y-axis representing the next largest.

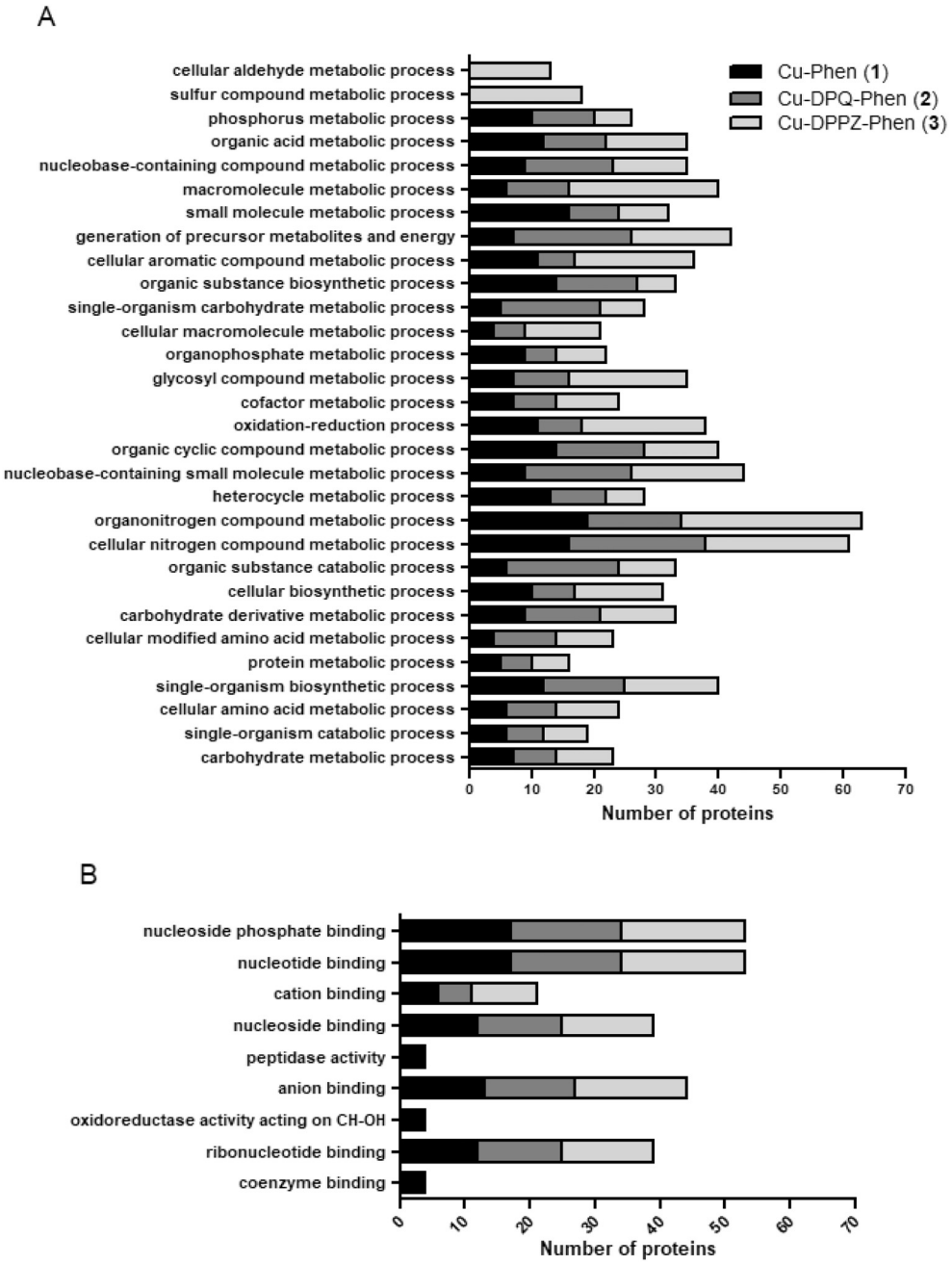

Fig. 4. Bar chart showing the different number of proteins present in a test exposure that is associated with selected biological processes **(A)** and molecular functions (**B**). Comparative bar chart represents level 4 ontology.

DPPZ-Phen (**3**). Analysis of molecular functions (Fig. 4(B)) also showed a similar trend of increasing number of proteins involved in the functionally categorised processes as the Cu(II) series progressed from Cu-Phen > Cu-DPQ-Phen > Cu-DPPZ-Phen. Proteins associated with coenzyme binding, oxidoreductases acting on CH-OH and peptidase activity was only associated with exposure of Cu-Phen (**1**), while all other protein groups were co expressed by all three test complexes. Glutathione *S*-transferase (GST) highlighted in the KEGG analysis (Fig. 5), exhibited an increased relative abundance following exposure to Cu-Phen (**1**), Cu-DPQ-Phen (**2**) and Cu-DPPZ-Phen (**3**) in comparison to the control. KEGG glycolysis/gluconeogenesis analysis (Fig. 6) of all three complex exposures showed an upregulation of several proteins: fructose bisphosphate, triose phosphate isomerase, glyceraldehydes-3-phosphate dehydrogenase and phosphopyruvate hydratase (enolase). KEGG analysis of purine metabolism (Fig. 7) showed increased relative abundance of 6 proteins after exposure to all test complexes: phosphoribosylaminoimidazolesuccinocarboxamide (SAICAR) synthase, phosphoribosylaminoimidazolecarboxamide (AICAR) formyltransferase, IMP cyclohydrolase, nucleoside-diphosphate kinase, nucleoside-triphosphate phosphatise and purine-nucleoside phosphorylase.

4. Discussion

The aim of this study was to assess the response of *G. mellonella* larvae to novel copper phenanthroline-phenazine complexes as a means to determine their biological mode of action and therefore developmental potential. Larval mortality decreased as the ligated phenazine ligand in the $[Cu(phen)(N,N')]^{2+}$ model was extended (Cu-Phen (**1**) > Cu-DPQ-Phen (**2**) > Cu-DPPZ-Phen (**3**)). The mortality assay demonstrates that the complex series had superior toxicity at all time-points to cisplatin with the exception of Cu-DPPZ-Phen (**3**) which, in comparison to Cu-Phen (**1**) and Cu-DPQ-Phen (**2**) was relatively non-toxic. Previous studies have confirmed the enhanced toxicity of copper complexes in comparison to platinum agents in *G. mellonella* larvae [42].

Immune priming often plays a large role in the larval response to foreign bodies, either chemical or pathological and alterations in the larval haemocyte density is one of the earliest markers of the invertebrate immune response [60]. Both controls and complex series induced a non-significant increase in the haemocyte response after complex exposure, which indicates that the novel Cu(II) complex series does not elicit a generalised cellular immune response. The non-stimulation of a non-specific immune response was also shown with the

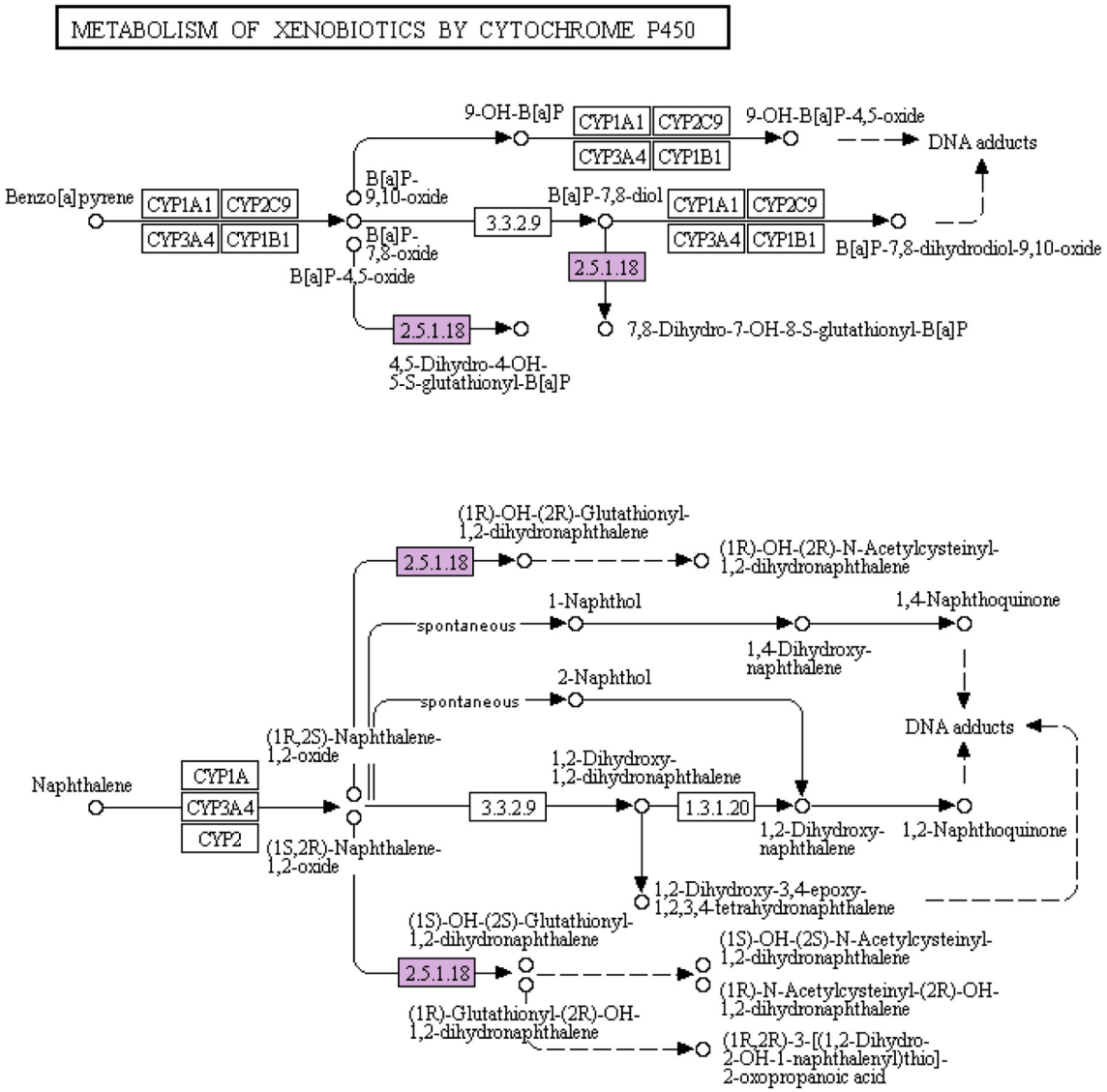

Fig. 5. KEGG analysis of the metabolism of selected xenobiotics by cytochrome P450. Glutathione *S*-transferase (2.5.1.18) (pink) is shown to be significantly upregulated in all test exposures.

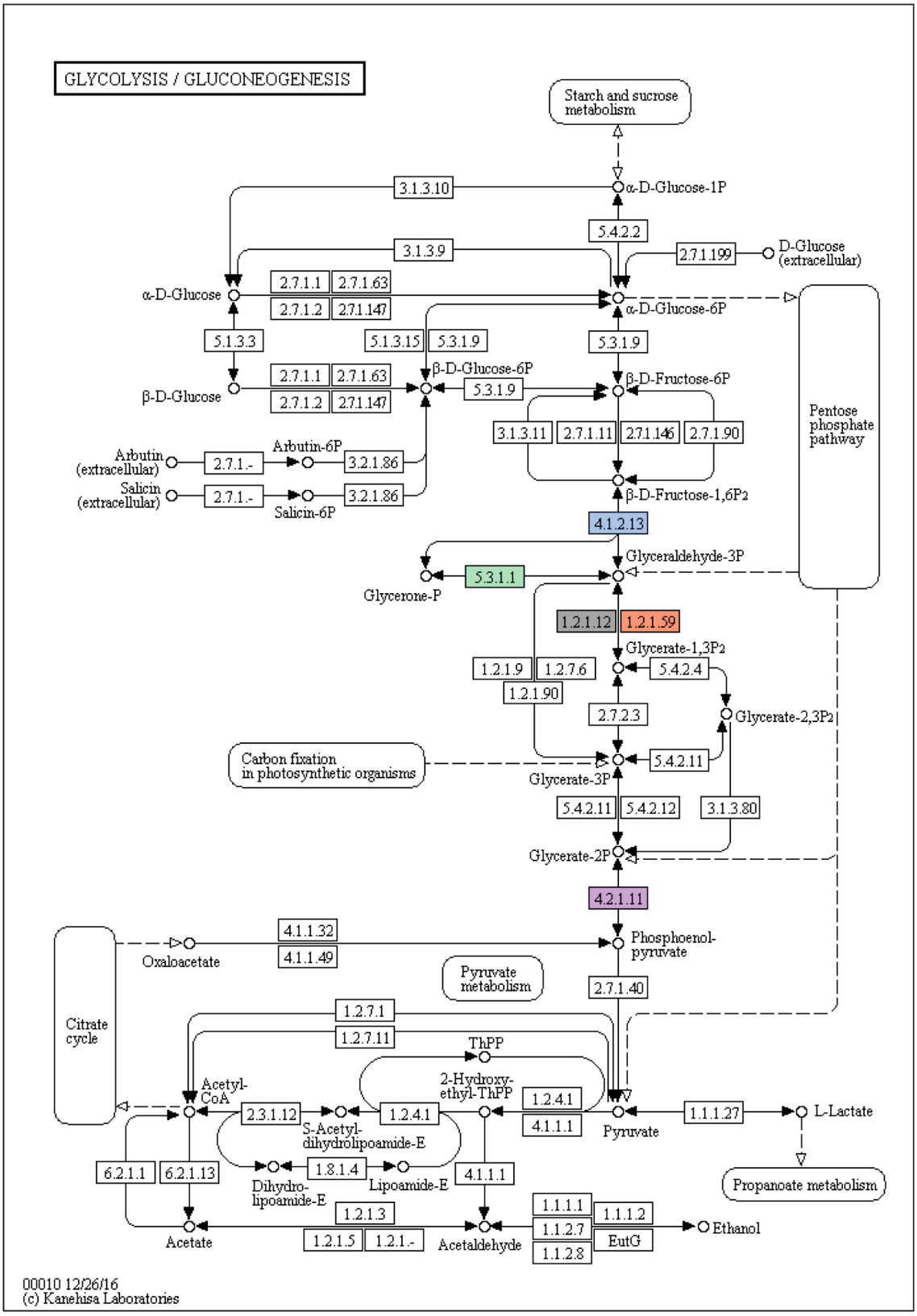

Fig. 6. KEGG analysis of significantly upregulated proteins in glycolysis/gluconeogenesis (highlighted: blue, green, grey, orange and pink) between all test exposures. Cu-DPQ-Phen (**2**) shows no upregulation of 4.2.1.11 (phosphopyruvate hydratase) (pink).

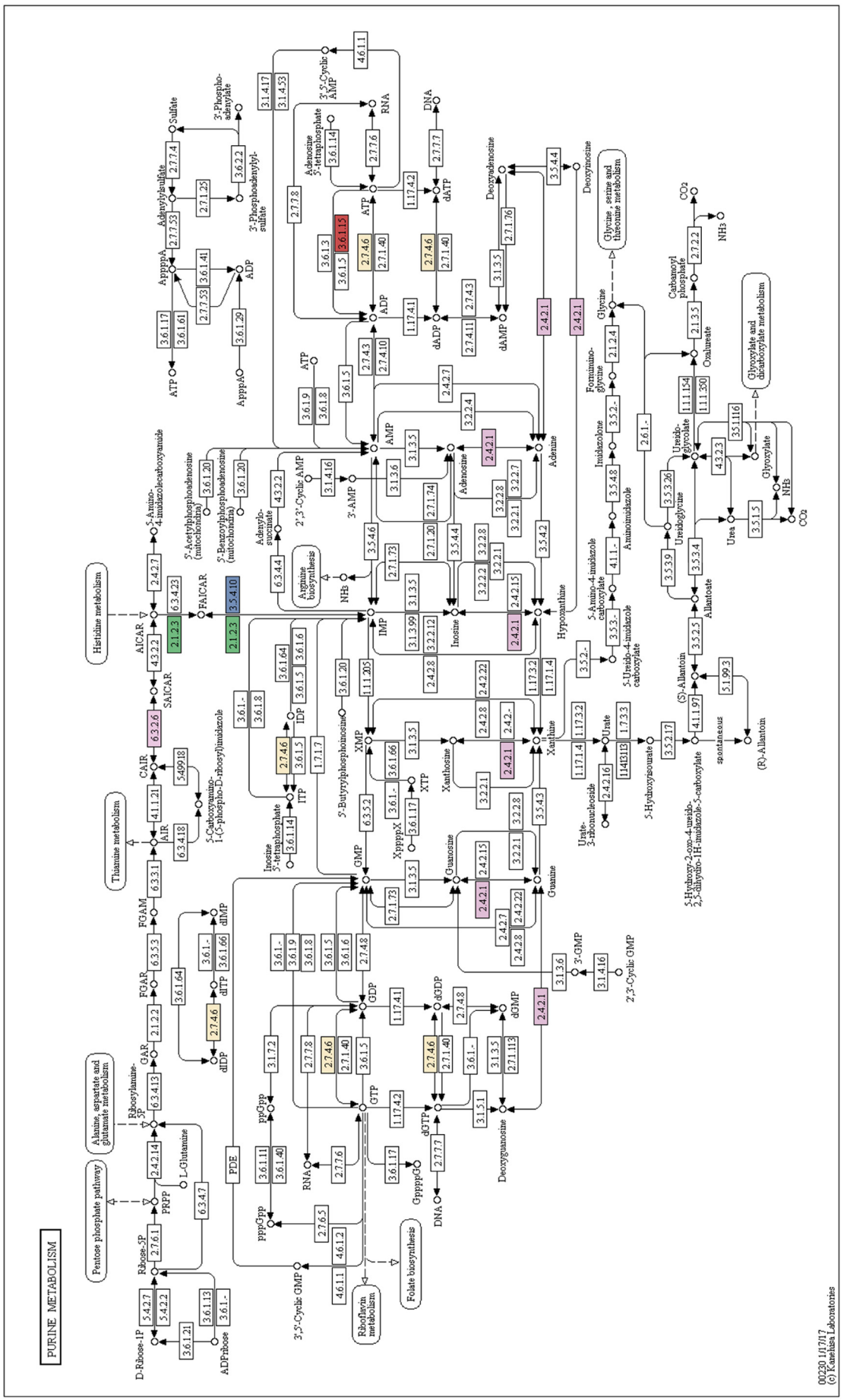

Fig. 7. KEGG analysis of significantly upregulated proteins in purine metabolism (highlighted: pink, yellow, green, blue and red) between all test exposure.

evaluation of the antimicrobial effects of 1,3-dibenzyl-4,5-diphenylimidazol-2-ylidene silver(I) acetate (SBC3) in *G. mellonella* post infection with *Staphylococcus aureus* and *Candida albicans* [44]. In contrast, other studies have shown a priming of the larval immune response with biologically derived echinocandines producing a resistance to subsequent infection [53]. The priming of the immune response has been previously observed through amplification of immune related genes [41, 54, 61]. This study in contrast shows significant decreases in IMPI and transferrin gene expression after exposure to the metallo-agents compared to the solvent control. Transferrin is typically increased following infection and based on functional homology with mammalian systems, sequesters biologically active iron from circulation to prevent it from being used as a microbial growth factor. IMPI was first identified in *G. mellonella* and is responsible for breaking down metal based proteases released by microbial pathogens [62]. Significantly, across the complex series there is no increase in either of these antimicrobial factors, indicating that at a cellular and messenger Ribonucleic Acid (mRNA) level, the Cu(II) complexes are not eliciting a larval immune response in a similar fashion to carbene silver(I) acetate (SBC3) exposure [44]. In contrast, the larval exposure to caspofungin induces an immune priming reaction [53].

In this study, LFQ proteomics produced a high-resolution analysis of the larval response to the complex series with the possibility of gaining an insight into the potential response in the mammalian system. Two-dimensional poly acrylamide gel electrophoresis (2D-PAGE) provides a lower resolution confirmation of several proteins detected in the LFQ proteomics. Using 2D-PAGE proteomics the downregulation of three proteins was confirmed in addition to 4 other detections of lower abundance proteins (Supplementary Table V-VI). Both 2D-PAGE and LFQ proteomics supports the finding of decreased immune response found in the immune related gene expression and the non-significant increase in the larval haemocyte response. 2D-PAGE analysis showed that imaginal disc growth factor and apolipophorin was downregulated in larvae treated with either Cu-DPQ-Phen (**2**) or Cu-DPPZ-Phen (**3**). Additionally, transferrin, juvenile like binding hormone and 27 kDa hemolymph protein was downregulated after exposure of larvae to Cu-DPPZ-Phen (**3**). All larvae were exposed to the 24 h LD_{50} value of the 3 complexes but have a different number of proteins significantly altered in abundance.

GST is a family of phase II detoxification enzymes that catalyses the conjugation of glutathione to a wide variety of endogenous and exogenous electrophilic compounds by making the exogenous molecule more hydrophilic, which aids in its elimination [63, 64]. Studies have shown GST abundance to be elevated during oxidative stress in the mammalian system [65]. Evidence has also linked the GST isozymes to anti-cancer drug resistance [66]. The action of copper *N*-(2-hydroxy acetophenone) glycinate has shown promise in overcoming doxorubicin generated GST and Multi Drug Resistance (MDR) [67]. KEGG analysis of the metabolism of xenobiotics by cytochrome P450 (Fig. 5) highlighted the involvement of GST in detoxification of benzo-[a]-pyrene and napthalene both of which contain polycyclic aromatic rings which are present in the phenazine ligand in Cu-DPQ-Phen (**2**) and Cu-DPPZ-Phen (**3**). The upregulation of GST is also involved in the detoxification of cyclophosphamide and ifosfamide which are key therapeutic alkylating agents. Cu-Phen (**1**), Cu-DPQ-Phen (**2**) and Cu-DPPZ-Phen (**3**) have previously been shown to have nuclease cleaving ability [32], and potentially interact with DNA through intercalation properties at the minor groove as seen with the ruthenium complex Λ-[Ru $(phen)_2dppz]^{2+}$ [68].

Cu-DPQ-Phen (**2**) and Cu-DPPZ-Phen (**3**) have previously been shown to generate excellent Superoxide Dismutase (SOD) mimetic activity with a progressive Fenton reaction matching the cadence of the chemical nuclease capacity against pUC19 DNA [32]. Mitochondrial aldehyde dehydrogenase and mitochondrial superoxide dismutase have been shown to be closely associated with oxidative stress [69, 70]. The upregulation of activity of these proteins in both the Cu-DPQ-Phen (**2**) and Cu-DPPZ-Phen (**3**) treated larvae may be associated with increased oxidative stress. Aldehyde dehydrogenase in mammalian cells has been associated with tolerance to increased organic nitrates [71], which are known to produce oxidative stress. The upregulation of both aldehyde dehydrogenase and superoxide dismutase in the Cu-DPQ-Phen (**2**) and Cu-DPPZ-Phen (**3**) treated larvae rather than just the upregulation of aldehyde dehydrogenase in the Cu-Phen (**1**) may indicate that oxidative stress plays a stronger mechanistic role in the secondary phenazine ligands despite the lower LD_{50} value. Isocitrate dehydrogenase is only upregulated in Cu-Phen (**1**) exposure while malate dehydrogenase is only upregulated in Cu-DPQ-Phen (**2**) and Cu-DPPZ-Phen (**3**) treated larvae. These dehydrogenases are closely linked to the Tricarboxylic Acid (TCA) cycle and have an effect on Nicotinamide Adenine Dinucleotide +/H (NAD+/NADH) ratio, which has been the subject of renewed interest due to its capacity to alter/ameliorate the effects on aging and other complex disease phenotypes [72]. An additional dehydrogenase present at increased levels of abundance in all exposures is 15-hydroxylprostaglandin dehydrogenase[NAD(+)] which has been shown to suppress eicosanoids such as prostaglandins and liposin, previously demonstrated to have anticancer properties [73].

KEGG analysis of glycolysis/gluconeogenesis (Fig. 6) indicated upregulation of fructose bisphosphate, triose phosphate isomerase, glyceraldehydes-3-phosphate dehydrogenase and phosphopyruvate hydratase (enolase) after exposure to all complexes. Previous studies have shown enolase to become up regulated in response to cellular stress [74]. Based on the study conducted by Molphy et al. [32], Cu(II) phenanthroline-phenazine complexes showed chemical nuclease activity in pUC19 plasmid DNA. Chemical nuclease action on larval DNA may have contributed to cellular stress and related alterations in carbohydrate metabolism. Glyceraldehyde-3-phosphate dehydrogenase was also highlighted and is involved in the conversion of glyceraldehydes-3-phosphate to D-glycerate. The non-enzymatic elimination of phosphate groups from glyceraldehyde-3-phosphate can lead to the production of the cytotoxic methylglyoxal which is known to be a progenitor of advanced glycation end-products [75].

Purine metabolism from KEGG analysis (Fig. 7) indicated increased abundance of regulatory enzymes SAICAR, AICAR and other purine support enzymes. Changes in purine metabolism as a result of cellular stress states have promoted increased interest recently as a potential therapeutic target for new drug development [76]. Among some of the new studies is evidence for the formation of a dynamic multi-enzyme complex (purinosome) proximal to the mitochondria and microtubules [77]. The formation of this multimeric protein complex has been associated with the depletion of purines and the upregulation of heat shock 90 protein (HSP90) which aids in higher order protein structure [76]. Based on the KEGG analysis, HSP90 was observed at higher levels of abundance in larvae treated with all test complexes highlighting the potential involvement of the newly described purinosome in the mechanistic response to nuclease active drugs due to accelerated DNA breakdown from the cleavage activity of the metal complexes.

The GO analysis demonstrated marked elevation in the following protein groups: cellular nitrogen compound metabolic process, organonitrogen compound metabolic process, heterocyclic metabolic process, organic cyclic compound metabolic process, organic substance biosynthetic process and small molecule metabolic process associated proteins. The increased abundance of proteins associated with the complex series and in particular, Cu-DPQ-Phen (**2**) and Cu-DPPZ-Phen (**3**) are accompanied by a broad upregulation in detoxification and degradation pathways. The increased abundance of nitrogen containing, heterocyclic and small molecule related metabolism most likely reflects the cellular detoxification response to the complexes which peaks upon administration with Cu-DPQ-Phen (**2**) and Cu-DPPZ-Phen (**3**). The GO analysis of molecular function at level 4 ontology showed an elevated group of proteins indicative of DNA binding by all the test complexes; nucleotide binding and nucleoside phosphate binding. The upregulated activity of these groups of proteins may reflect an

increased association with DNA damage and potential repair complexes. Radical hydroxyl attack is believed to be an effect of these complexes owing to their previously established Fenton chemistry [32].

5. Conclusion

This investigation showed that the extension of the phenazine π-backbone within the complex scaffold resulted in a decrease in both mortality and immune response in the larval model with the trend following Cu-Phen < Cu-DPQ-Phen < Cu-DPPZ-Phen. Similarly to previous studies, enhanced toxicity is observed with increased nuclease capacity, however in contrast enhanced DNA binding and thermal melting stability governed by the extended phenazine π-framework results in a decrease in mortality here [16, 78].

The label free quantitation (LFQ) mass spectrometry method produced a high-resolution assessment of the proteomic changes occurring in the larvae in response to test complexes allowing for gene ontology (GO) analysis of both biological and molecular functions to be performed. The results indicated a prominent metabolic and detoxification response which may provide an opportunity to develop drug targeting to this region but also to utilise the larval model to evaluate future therapeutic and targeting improvements.

Acknowledgments

The authors would like to thank the Dublin Institute of Technology (DIT) for providing the Fiosraigh funding (funding call 2013) for this research project. Q-Exactive mass spectrometer was funded under the SFI Research Infrastructure Call 2012; Grant Number: 12/RI/2346 (3). ZM acknowledges support by Irish Research Council (IRC) grant GOIPG/2013/826.

Financial disclosures

Authors have no financial conflicts to disclose.

Conflicts of interest

Authors have none to declare.

Appendix A. Supplementary data

Supplementary data to this article can be found online at https://doi.org/10.1016/j.jinorgbio.2018.05.020.

References

[1] H. Song, J.T. Kaiser, J.K. Barton, Nat. Chem. 4 (2012) 615–620.
[2] H. Niyazi, J.P. Hall, K. O'Sullivan, G. Winter, T. Sorensen, J.M. Kelly, C.J. Cardin, Nat. Chem. 4 (2012) 621–628.
[3] J.P. Hall, D. Cook, S.R. Morte, P. McIntyre, K. Buchner, H. Beer, D.J. Cardin, J.A. Brazier, G. Winter, J.M. Kelly, C.J. Cardin, J. Am. Chem. Soc. 135 (2013) 12652–12659.
[4] A.J. McConnell, H. Song, J.K. Barton, Inorg. Chem. 52 (2013) 10131–10136.
[5] C.J. Cardin, J.M. Kelly, S.J. Quinn, Chem. Sci. 8 (2017) 4705–4723.
[6] J. Chen, J. Stubbe, Nat. Rev. Cancer 5 (2005) 102–112.
[7] J. Malina, M.J. Hannon, V. Brabec, Chem. Eur. J. 21 (2015) 11189–11195.
[8] S.J. Berners-Price, A. Filipovska, Metallomics 3 (2011) 863–873.
[9] T. Zou, C.T. Lum, C.-N. Lok, J.-J. Zhang, C.-M. Che, Chem. Soc. Rev. 44 (2015) 8786–8801.
[10] Z. Du, R.E.F. de Paiva, K. Nelson, N.P. Farrell, Angew. Chem. Int. Ed. 56 (2017) 4464–4467.
[11] A. Prisecaru, M. Devereux, N. Barron, M. McCann, J. Colleran, A. Casey, V. McKee, A. Kellett, Chem. Commun. 48 (2012) 6906–6908.
[12] A. Kellett, O. Howe, M. O'Connor, M. McCann, B.S. Creaven, S. McClean, A. Foltyn-Arfa Kia, A. Casey, M. Devereux, Free Radic. Biol. Med. 53 (2012) 564–576.
[13] M. McCann, J. McGinley, K. Ni, M. O'Connor, K. Kavanagh, V. McKee, J. Colleran, M. Devereux, N. Gathergood, N. Barron, A. Prisecaru, A. Kellett, Chem. Commun. 49 (2013) 2341–2343.
[14] C. Santini, M. Pellei, V. Gandin, M. Porchia, F. Tisato, C. Marzano, Chem. Rev. 114 (2014) 815–862.
[15] R. Larragy, J. Fitzgerald, A. Prisecaru, V. McKee, P. Leonard, A. Kellett, Chem. Commun. 51 (2015) 12908–12911.
[16] C. Slator, N. Barron, O. Howe, A. Kellett, ACS Chem. Biol. 11 (2016) 159–171.
[17] C. Marzano, M. Pellei, F. Tisato, C. Santini, Anti Cancer Agents Med. Chem. 9 (2009) 185–211.
[18] S. Tardito, L. Marchio, Curr. Med. Chem. 16 (2009) 1325–1348.
[19] F. Tisato, C. Marzano, M. Porchia, M. Pellei, C. Santini, Med. Res. Rev., 30, 708–749.
[20] N.P. Farrell, Chem. Soc. Rev. 44 (2015) 8773–8785.
[21] A. Gupta, S. Lutsenko, Future Med. Chem. 1 (2009) 1125–1142.
[22] R. Galindo-Murillo, J.C. García-Ramos, L. Ruiz-Azuara, T.E. Cheatham, F. Cortés-Guzmán, Nucleic Acids Res. 43 (2015) 5364–5376.
[23] C. Mejia, L. Ruiz-Azuara, Pathol. Oncol. Res. 14 (2008) 467–472.
[24] C. Trejo-Solís, G. Palencia, S. Zuñiga, A. Rodríguez-Ropon, L. Osorio-Rico, S. Torres Luvia, I. Gracia-Mora, L. Marquez-Rosado, A. Sánchez, M.E. Moreno-García, A. Cruz, M.E. Bravo-Gómez, L. Ruiz-Ramírez, S. Rodríquez-Enriquez, J. Sotelo, Neoplasia 7 (2005) 563–574.
[25] F. Carvallo-Chaigneau, C. Trejo-Solís, C. Gómez-Ruiz, E. Rodríguez-Aguilera, L. Macías-Rosales, E. Cortés-Barberena, C. Cedillo-Peláez, I. Gracia-Mora, L. Ruiz-Azuara, V. Madrid-Marina, F. Constantino-Casas, Biometals 21 (2008) 17–28.
[26] M.E. Bravo-Gómez, C. Campero-Peredo, D. García-Conde, M.J. Mosqueira-Santillán, J. Serment-Guerrero, L. Ruiz-Azuara, Polyhedron 102 (2015) 530–538.
[27] D.S. Sigman, D.R. Graham, V. D'Aurora, A.M. Stern, J. Biol. Chem. 254 (1979) 12269–12272.
[28] D.S. Sigman, Acc. Chem. Res. 19 (1986) 180–186.
[29] D.S. Sigman, T.W. Bruice, A. Mazumder, C.L. Sutton, Acc. Chem. Res. 26 (1993) 98–104.
[30] C. Slator, Z. Molphy, V. McKee, C. Long, T. Brown, A. Kellett, Nucleic Acids Res. (2018), http://dx.doi.org/10.1093/nar/gky105.
[31] A. Prisecaru, V. McKee, O. Howe, G. Rochford, M. McCann, J. Colleran, M. Pour, N. Barron, N. Gathergood, A. Kellett, J. Med. Chem. 56 (2013) 8599–8615.
[32] Z. Molphy, A. Prisecaru, C. Slator, N. Barron, M. McCann, J. Colleran, D. Chandran, N. Gathergood, A. Kellett, Inorg. Chem. 53 (2014) 5392–5404.
[33] G. Cotter, S. Doyle, K. Kavanagh, FEMS Immunol. Med. Microbiol. 27 (2000) 163–169.
[34] K. Kavanagh, E.P. Reeves, FEMS Microbiol. Rev. 28 (2004) 101–112.
[35] M. Kemp, R.C. Massey, Drug Discov. Today 4 (2007) 105–110.
[36] K. Kavanagh, J.P. Fallon, Fungal Biol. Rev. 24 (2010) 79–83.
[37] N. Browne, M. Heelan, K. Kavanagh, Virulence 4 (2013) 597–603.
[38] J. Renwick, K. Kavanagh, Kevin Kavanagh (Ed.), New Insights in Medical Mycology, 1 Springer, Netherlands, 2007, pp. 45–67 Ch. 2.
[39] S.M. Cook, J.D. McArthur, Virulence 4 (2013) 350–353.
[40] D. Bergin, E.P. Reeves, J. Renwick, B. Frans, K. Kavanagh, F.B. Wientjes, Infect. Immun. 73 (2005) 4161–4170.
[41] D. Bergin, L. Murphy, J. Keenan, M. Clynes, K. Kavanagh, Microbes Infect. 8 (2006) 2105–2112.
[42] M. McCann, A.L.S. Santos, B.a. da Silva, M.T.V. Romanos, A.S. Pyrrho, M. Devereux, K. Kavanagh, I. Fichtner, A. Kellett, Toxicol. Res. 1 (2012) 47.
[43] M. McCann, R. Curran, M. Ben-Shoshan, V. McKee, M. Devereux, K. Kavanagh, A. Kellett, Polyhedron 56 (2013) 180–188.
[44] N. Browne, F. Hackenberg, W. Streciwilk, M. Tacke, K. Kavanagh, Biometals 27 (2014) 745–752.
[45] A. Kellett, M. O'Connor, M. McCann, O. Howe, A. Casey, P. McCarron, K. Kavanagh, M. McNamara, S. Kennedy, D.D. May, P.S. Skell, D. O'Shea, M. Devereux, Med. Chem. Commun. 2 (2011) 569–676.
[46] Z. Molphy, C. Slator, C. Chatgilialoglu, A. Kellett, Front. Chem. 3 (2015) 1–9.
[47] A. D'Alessandro, S. Rinalducci, L. Zolla, J. Proteome 74 (2011) 2575–2595.
[48] Y. Wang, J.F. Chiu, Metal-Based Drugs (2008), http://dx.doi.org/10.1155/2008/716329.
[49] G. Cotter, S. Doyle, K. Kavanagh, FEMS Immunol. Med. Microbiol. 27 (2000) 163–169.
[50] N. Browne, C. Surlis, K. Kavanagh, J. Insect Physiol. 63 (2014) 21–26.
[51] L. Vertyporokh, I. Wojda, Acta Biochim. Pol. 64 (2016) 6.
[52] T. Yoshiga, T. Georgieva, B.C. Dunkov, N. Harizanova, K. Ralchev, J.H. Law, Eur. J. Biochem. 260 (1999) 414–420.
[53] J. Kelly, K. Kavanagh, J. Med. Microbiol. 60 (2011) 189–196.
[54] I. Wojda, T. Jakubowicz, J. Insect Physiol. 53 (2007) 1134–1144.
[55] R. Maguire, M. Kunc, P. Hyrsl, K. Kavanagh, Comp. Biochem. Physiol., Part C: Toxicol. Pharmacol. 195 (2017) 44–51.
[56] A. Shevchenko, H. Tomas, J. Havlis, J.V. Olsen, M. Mann, Nat. Protoc. 1 (2006) 2856–2860.
[57] J. Cox, N. Neuhaurser, A. Michalskit, R.A. Scheltema, J.V. Olsen, M. Mann, J. Proteome Res. 10 (2011) 1794–1805.
[58] H. Vogel, B. Altincicek, G. Glöckner and A. Vilcinskas, BMC Genomics, 2011, 12, DOI: 1471–2164/12/308.
[59] K.J. Livak, T.D. Schmittgen, Methods 25 (2001) 402–408.
[60] N. Browne, An Analysis of the Cellular and Humoral Immune Responses of Galleria Mellonella Larvae, Maynooth University, 2014.
[61] A.N. Volkoff, J. Rocher, E. D'Alençon, M. Bouton, I. Landais, E. Quesada-Moraga, A. Vey, P. Fournier, K. Mita, G. Devauchelle, Gene 319 (2003) 43–53.
[62] M. Wedde, C. Weise, P. Kopacek, P. Franke, A. Vilcinskas, Eur. J. Biochem. 255 (1998) 535–543.
[63] D. Bartolini, J. Commodi, M. Piroddi, L. Incipini, L. Sancineto, C. Santi, F. Galli, Free Radic. Biol. Med. 88 (2015) 466–480.
[64] A.A. Enayati, H. Ranson, J. Hemingway, Insect Mol. Biol. 14 (2005) 3–8.
[65] P.G. Board, D. Menon, Biochim. Biophys. Acta 1830 (2013) 3267–3288.

[66] D.M. Townsend, K.D. Tew, Oncogene 22 (2003) 7369–7375.
[67] S. Majumder, P. Dutta, A. Mookerjee, S.K. Choudhuri, Chem. Biol. Interact. 159 (2006) 90–103.
[68] H. Niyazi, J. Hall, K. O'Sullivan, G. Winter, T. Sorensen, J. Kelly, C. Cardin, Nat. Chem. 4 (2012) 621–628.
[69] A. Daiber, Mol. Pharmacol. 66 (2004) 1372–1382.
[70] J. McCord, I. Fridovich, Free Radic. Biol. Med. 5 (1988) 363–369.
[71] Z. Chen, J. Zhang, J.S. Stamler, Proc. Natl. Acad. Sci. U. S. A. 99 (2002) 8306–8311.
[72] Y. Yang, A.A. Sauve, Biochim. Biophys. Acta 1864 (2016) 1787–1800.
[73] S. Tuncer, S. Banerjee, World J. Gastroenterol. 21 (2015) 11748–11766.
[74] H. Ji, J. Wang, J. Guo, Y. Li, S. Lian, W. Guo, H. Yang, F. Kong, L. Zhen, L. Guo, Y. Liu, Anim. Nutr. Health 2 (2016) 12–17.
[75] I. Allaman, M. Bélanger, P.J. Magistretti, Front. Neurosci. 9 (2015) 1–12.
[76] I. Chitrakar, D.M. Kim-Holzapfel, W. Zhou, J.B. French, J. Struct. Biol. 197 (2017) 354–364.
[77] A.M. Pedley, S.J. Benkovic, Trends Biochem. Sci. 42 (2017) 141–154.
[78] M. Devereux, M. McCann, D. O'Shea, M. O'Connor, E. Kiely, V. McKee, D. Naughton, A. Fisher, A. Kellett, M. Walsh, D. Egan, C. Deegan, Bioinorg. Chem. Appl. (2005), http://dx.doi.org/10.1155/BCA/2006/80283.